JOURNAL OF CATALYSIS 118, 31–42 (1989)

Luminescence Probes of Vanadium-Contaminated Fluid Cracking Catalysts

MICHAEL W. ANDERSON,* MARIO L. OCCELLI,† AND STEVEN L. SUIB*,[1]

*Department of Chemistry, University of Connecticut, Storrs, Connecticut 06268, and †UNOCAL Corporation, Science and Technology Division, Brea, California 92621

Received November 2, 1988; revised January 17, 1989

Vanadium deactivation and tin passivation of vanadium impurities in a model fluid cracking catalyst system consisting of an europium-exchanged Y zeolite and an amorphous aluminosilicate gel have been studied by luminescence techniques. Vanadium is found to be preferentially adsorbed by the gel and does not migrate after deposition and calcination but does migrate between the zeolite and the matrix during steaming. After heating in air at 575°C, vanadium is in the form of VO^{2+} cations on the zeolite and primarily in the form of V_2O_5 on the gel. The environment of Eu^{3+} cations is found to be very sensitive to heat treatment but not to the order of tin and vanadium deposition. Upon steaming, $EuVO_4$ is formed on the zeolite and this formation is promoted by the presence of excess Sn.

INTRODUCTION

More than 40 years after its introduction, fluidized cracking of petroleum fractions is still the main process of large-scale gasoline production (*1*). This process uses catalysts typically formed by spray drying an aluminosilicate slurry to which a clay mineral (like Kaolin) and a zeolite with the faujasite structure such as hydrogen Y (HY), or calcined rare-earth-exchanged Y (CREY), have been added in order to impart to the catalyst the desired physical properties and cracking activity characteristics.

Since the energy market is very competitive, refiners are interested in processing cheaper and more readily available metal-contaminated crudes and residual oils. These contaminated feedstocks deposit metals (Ni and Fe) on the catalyst surface which catalyze undesirable secondary cracking reactions. Metals such as V (and Cu) which reduce cracking activity are also deposited. Antimony organic complexes have been used to passivate Ni by drastically reducing hydrogen and coke formation generated by this metal (*2*, *3*). Tin is believed (*4*) capable of passivating V; however, little is known of Sn–V interactions.

In an effort to explain metal–surface interactions on cracking catalysts, luminescence experiments have been performed with V-loaded aluminosilicate gels and Eu^{3+}-exchanged Y (EuY) zeolites in the presence of a passivating agent such as Sn. Eu^{3+} was chosen in place of the more common La^{3+} or Ce^{3+} because Eu^{3+} cations are efficient emitters and luminescence spectral data can yield information on their environment (*10*).

EXPERIMENTAL

Sample Preparation

Ammonium zeolite Y (Linde LZY-62) was exchanged with Eu^{3+} cations by stirring 4 g of zeolite in 400 ml of 0.05 *M* $Eu(NO_3)_3$ at room temperature for 24 hr; the pH of the exchange solution was 5.3. After exchange, the zeolite was washed sparingly with water to remove excess nitrates and dried in air at room temperature. AAA-alumina, a gel consisting of 70 wt% SiO_2, 30 wt% Al_2O_3, was obtained from Davison, Columbia, Maryland. A third

[1] To whom correspondence should be addressed.

0021-9517/89 $3.00

sample was prepared by making a 50/50 mixture of EuY and AAA-alumina with a mortar and pestle.

The EuY was loaded with 1 wt% Sn using a hot solution of tetraphenyltin (ALFA Ventron) dissolved in toluene. Excess toluene was removed under reduced pressure and the resulting solid was calcined at 575°C in flowing air for 12 hr to remove the phenyl ligands. A second incipient wetness treatment was performed to load the zeolite with 1 wt% vanadium from a solution of vanadyl naphthenate (Pfaltz and Bauer) in toluene. Again, this was followed by a similar calcination step. Finally, the zeolite was steam deactivated by heating to 730°C for 10 hr with 95% steam/5% N_2 at a flow rate of 4 ml liquid water per hour. Such a treatment of EuY will be abbreviated by using the mnemonic qualifier SNCVCS: SN, 1 wt% tin loading; C, calcination; V, 1 wt% vanadium loading; S, steaming. At intermediate stages of treatment, the qualifier will be shorter; i.e., EuY (SNC) signifies tin loading followed by calcination. The order of metal loading has also been reversed and different Sn concentrations used. Finally, mixtures of EuY and gel were prepared after various stages of treatment. For instance, after loading tin onto EuY, the gel was added before calcination. Such a sample would be referred to as EuY (SNAAAC). Mixing of the two components was also performed prior to metal addition (EuY/AAA). Table 1 gives a listing of all the sample treatments with abbreviations

TABLE 1

Sample Designations

Substrate	Sn 1st	V 1st	AAA added prior to calc.	EuY added prior to calc.	Sn 2nd	V 2nd	AAA added prior to calc.	EuY added prior to calc.	Design.[a]
EuY	X					X			SNCVCS
		X			X				VCSNCS
	X		X						SNAAACS
	X						X		SNCAAAS
		X	X						VAAACS
		X					X		VCAAAS
	X								SNCS
		X							VCS
AAA	X					X			SNCVCS
		X			X				VCSNCS
	X			X					SNYCS
	X							X	SNCYS
		X		X					VYCS
		X						X	VCYS
	X								SNCS
		X							VCS
EuY/AAA	X					X			SNCVCS
		X			X				VCSNCS
	X								SNCS
		X							VCS

[a] SN, tin loading; V, vanadium loading; C, calcination; S, steaming; Y, mixed with EuY; AAA, mixed with AAA-alumina.

used throughout the text. A flow diagram of the different stages of sample treatment is given in Scheme I.

Luminescence

Both excitation and emission spectra were recorded using a Spex Fluorolog 202B double monochromator fluorescence spectrometer. The spectrometer was operated in the front-face mode with bandpass slits of 0.9 nm for europium luminescence and 2.7 nm for vanadium luminescence. Excitation spectra were recorded using a Rhodamine B solution as a reference to correct for variations in the arc lamp intensity. Spectra were recorded at 77 K by sealing the sample in an evacuated quartz tube which was placed in a liquid nitrogen Dewar. This was necessary to monitor phosphorescence from V_2O_5.

Luminescence Lifetime

Luminescence lifetime measurements were made with a PRA Model 3000 system. A PRA Model LN102 nitrogen laser pulsing at 20 Hz with a pulse width of 300 ps was used as an excitation source. Either the direct laser output at 337 nm was used or the excitation wavelength was tuned with a dye to give maximum output at 390 nm. Data were collected on a Tracor–Northern multichannel analyzer and were transferred to a Digital Corp. PDP-1103 computer for storage and fitting. Statistical analysis was performed using the software packaging Decay 3.0 purchased from PRA Corp.

RESULTS

Room-temperature luminescence was used to observe the Eu^{3+} cation while 77 K luminescence was used to detect vanadia. The intensity ratios of all relevant luminescence bands are given in Table 2. Figure 1 shows the excitation and emission spectra of "fresh" EuY. The excitation spectrum was independent of the emission band chosen for observation and consists of a strong band at 393 nm with very weak bands at 375, 464, and 525 nm. In most of the subsequent work, the 616-nm emission band was chosen for collection of excitation spectra.

The EuY emission spectrum shows three main bands at 592, 616, and 699 nm (Fig. 1a). The same three main bands are present in the emission spectrum of calcined EuY; however, the intensity ratios of the bands have changed and also the weak band at 650 nm is enhanced (Fig. 2a). Additionally, fine

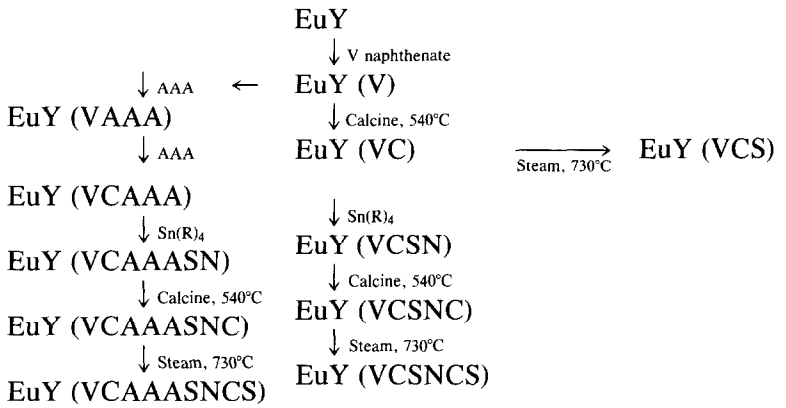

SCHEME I. Representation scheme for sample preparation. Note: the above pathways are only two of the possible routes of preparation used in this research and both are from a EuY starting point. The other two starting points are AAA and a premixed EuY/AAA mixture. The above paths are for V addition prior to Sn addition. The work described in this paper also involves addition of Sn first followed by V addition. Specific abbreviations are as follows: AAA, AAA-alumina; EuY, Eu-exchanged NH_4Y zeolite; V, vanadium naphthenate; SN, tetraphenyl tin; R, phenyl; C, calcination; S, steam treatment.

TABLE 2

Relative Intensities of Excitation and Emission Bands

	Emission				Excitation			
	597	622	650	700	396	465	532	330
Sample								
EuY	1.2	1	0	0.7	1	0.1	0	a
C	0.6	1	0.1	0.4	1	0.3	0.3	a
V	a	a	a	a	a	a	a	a
VC	0	a	0	0	a	a	a	a
VCSNC	0.4	1	0.1	0.3	1	0.7	0.9	a
SNC	0.4	1	0.1	0.3	1	0.4	0.4	a
SNCVC	0.3	a	0.1	0.3	1	0.4	0.5	a
AAA/EuY VC	0.3	1	0.1	0.3	1	0.4	0.6	a
SNC	0.5	1	0.1	0.3	1	0.4	0.6	a
VCSNC	0.4	1	0.1	0.3	1	1.1	1.1	a
SNCVC	0.4	1	0.1	0.4	1	0.3	0.5	a
AAA V/EuYC	0.3	1	0	0.1	1	0.6	0.6	a
Steamed samples								
No V, no AAA	0.3	1	0.1	0.2	1	0.6	0.5	a
AAA, no V	0.3	1	0.1	0.2	1	0.4	0.3	a
V	0.3	1	0.1	0.2	1	1	1	10
AAA VC/EuY	0.3	1	0.1	0.2	1	1	1	5

(a) Weak, difficult to observe.

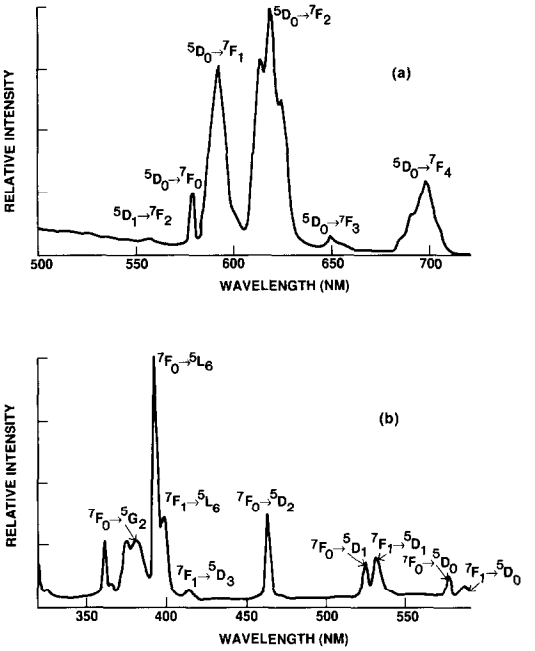

FIG. 2. Luminescence spectra for calcined EuY. (a) Emission with excitation wavelength at 393 nm; (b) excitation with emission wavelength at 616 nm.

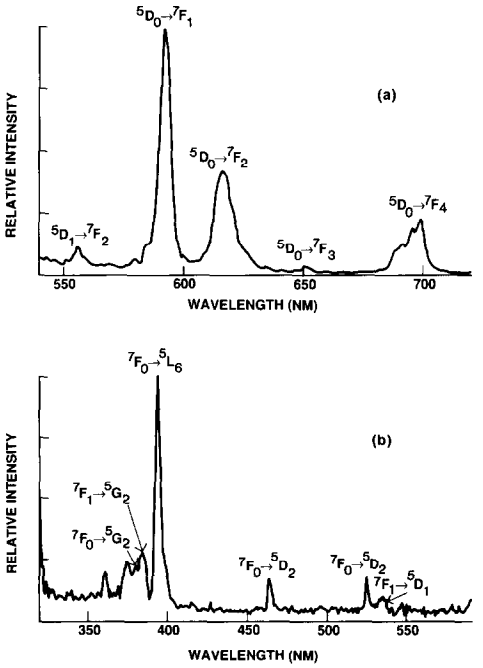

FIG. 1. Luminescence spectra for hydrated EuY. (a) Emission with excitation wavelength at 393 nm; (b) excitation with emission wavelength at 616 nm.

structure is now observed in the 616-nm band and a weak band is observed at 578 nm. More significantly, the excitation spectrum shown in Fig. 2b now has numerous bands that are clearly resolved. The main band is still at 393 nm but the 464-nm band is more intense and additional bands at 398, 532, 577, and 587 nm are also observed.

After addition of tin followed by calcination, the emission and excitation spectra are very similar to those for samples without tin (see Table 2 and Fig. 3a). However, after vanadium addition, the Eu^{3+} luminescence is almost completely quenched (Fig. 3b). Calcination restores only a fraction of the signal at 616 nm. In the excitation spectrum of this sample, EuY (SNCVC), an additional band at 320 nm is present (Fig. 3c). This band is always observed after calcination when vanadium is present on the zeolite.

When the V-loaded AAA-alumina is mixed with EuY and then calcined, the excitation spectrum shown in Fig. 4b is ob-

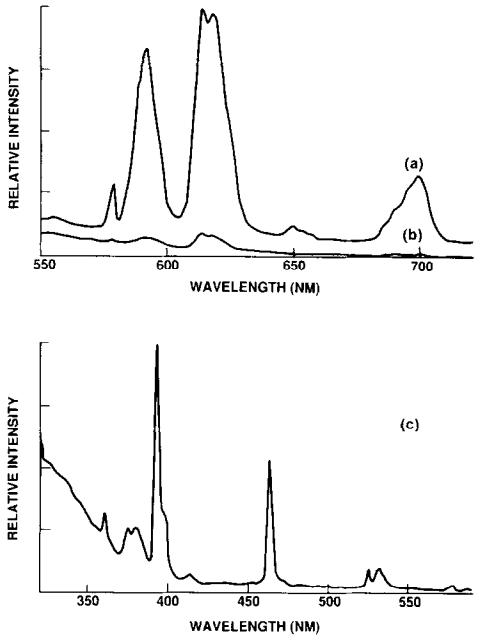

FIG. 3. Luminescence emission spectra with excitation wavelength at 393 nm for (a) EuY (SNC) and (b) EuY (SNCV). (c) Excitation spectrum for EuY (SNCVC) with emission wavelength at 616 nm.

tained. All the usual excitation bands are present and their intensities are comparable with those for calcined EuY. Figure 4a shows the excitation spectrum for AAA (VCYS). In this case, vanadium was deposited on the gel and calcined before adding the zeolite; the mixture was then steamed. This results in an additional intense broad band at 320 nm.

Calcined V-loaded zeolite [EuY (VC)] showed almost no luminescence and the spectrum remained unchanged after Sn addition. After calcination, an emission spectrum (Fig. 5) similar to that for calcined EuY (SNCVC) was obtained. The corresponding excitation spectrum shows a marked increase in the relative intensity of the 464-nm band relative to EuY (VCSNC) in Fig. 3c. Similar spectra were obtained for samples EuY (SNCVC) and AAA/EuY mixtures (VCSNC) and (SNCVC) suggesting that, in this case, the order of deposition of tin and vanadium is of little consequence with respect to the Eu^{3+} environment. In all

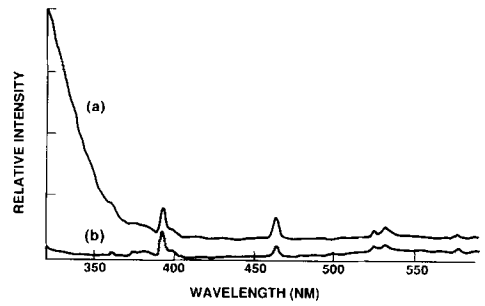

FIG. 4. Luminescence excitation spectra with emission wavelength at 616 nm for (a) AAA (VCYS) and (b) AAA (VCY).

V-free samples tin did not affect the europium luminescence, nor did calcination of the Sn-loaded materials.

Figure 6a shows the emission spectrum for EuY after calcination and steaming. Small changes in the relative intensity of the bands from calcined EuY are observed. Similarly, changes in the relative intensity of the excitation bands are apparent with the relative intensity of the 464-nm and 532-nm bands increasing significantly (see Table 2 and Fig. 6b).

Luminescence spectra for all the steamed samples fall into three categories best illustrated by consideration of their excitation spectra. First, there are the V-free EuY samples. These are exemplified by Fig. 6b for calcined and steamed EuY. The only other sample which falls into this category is EuY (SNCS). For these samples the ratio of intensities of the 393 : 464 : 531-nm bands

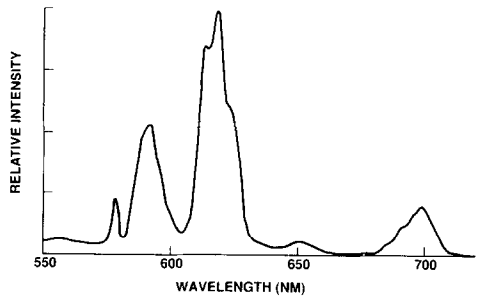

FIG. 5. Luminescence emission spectra with excitation wavelength at 393 nm for EuY (VCSNC).

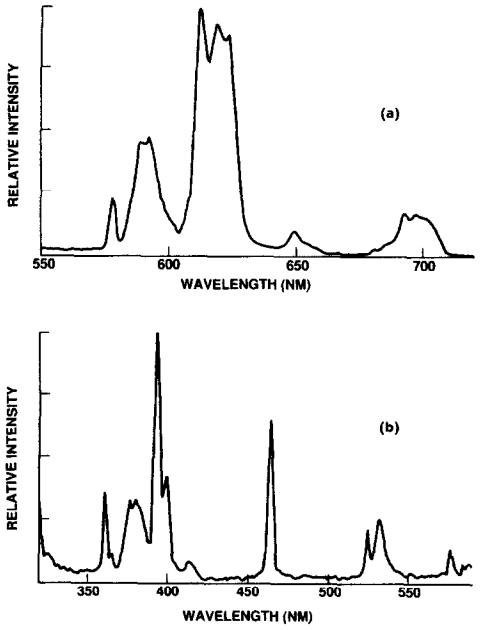

FIG. 6. Luminescence spectra for EuY (CS). (a) Emission spectrum with excitation wavelength at 393 nm; (b) excitation spectrum with emission wavelength at 616 nm.

is about 1.0:0.65:0.20. The second category contains V-free AAA-alumina (Fig. 7a). A similar ratio of peak intensities is about 1.0:0.80:0.26. The final class of steamed samples contains vanadium. Figure 7b shows the luminescence spectrum for EuY (SNCVCS). An additional broad peak is observed with maximum intensity near 320 nm and extending beyond 360 nm. The ratio of intensities of the 320:393:464:525-nm bands is about 7.0:1.0:0.80:0.30. The broad band centered at 320 nm is a feature of the same europium species because the same emission spectrum is obtained when exciting at 320, 464, and 525 nm.

The only exception to the above classification is AAA (VCYS) where the EuY was mixed with the vanadium-loaded AAA-alumina immediately prior to steaming. In this case, the four peaks are still observed at the wavelengths noted for the above-mentioned vanadium-containing systems but the ratio of the intensities of the peaks is 3.0:1.0:0.80;0.30 indicating that the intensity of the 320-nm band is diminished relative to the other bands. All steamed samples gave emission spectra similar to those shown in Fig. 6a. Excitation at the wavelengths of all the different excitation bands gave emission spectra similar to that shown in Fig. 6a. The effects of Sn concentration on the intensity of the luminescence signals for steamed vanadium-loaded EuY samples are illustrated in Fig. 8. The intensity of the europium luminescence increases with Sn concentration such that if the relative intensity is 1.0 with no Sn present, then for 1, 1.5, and 2.0 wt% Sn the relative intensities are 1.3, 7.1, and 13.6, respectively. Luminescence lifetimes for all these samples (with excitation at 337 nm and emission at 620 nm) are about 850 μs.

Figure 9 shows both the emission and the excitation spectra for a sample of $EuVO_4$ prepared by heating a stoichiometric amount of Eu_2O_3 and V_2O_5. The emission spectrum exhibits very sharp lines, the most intense being at 620 and 616 nm (Fig.

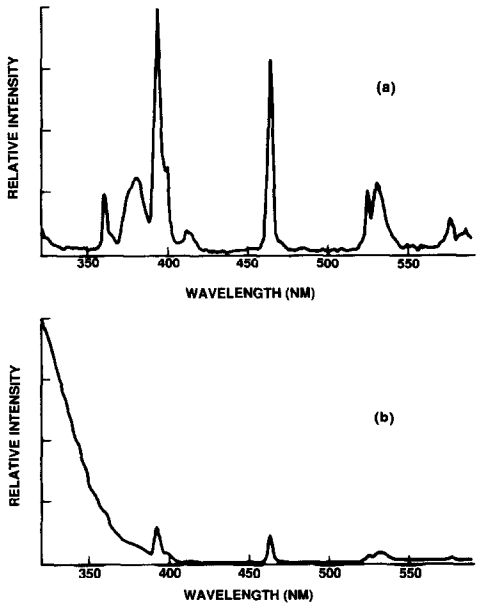

FIG. 7. Luminescence excitation spectra with emission wavelength at 616 nm for (a) AAA (SNCYC) and (b) EuY (SNCVCS).

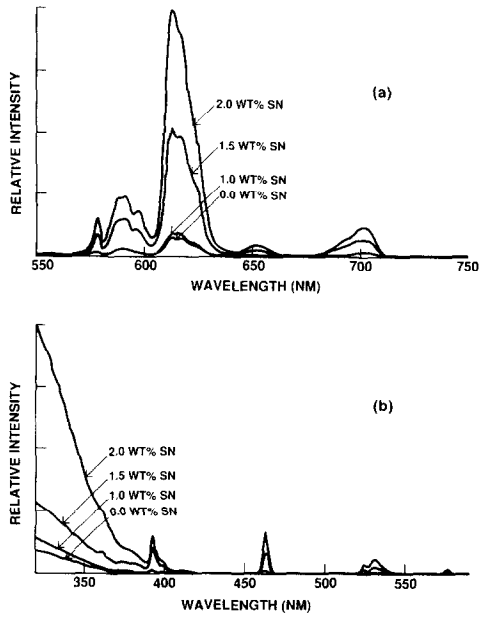

FIG. 8. Luminescence spectra for EuY containing 1 wt% V and varying concentrations of Sn after steaming. (a) Emission spectrum with excitation at 393 nm; (b) excitation spectrum with emission wavelength at 616 nm.

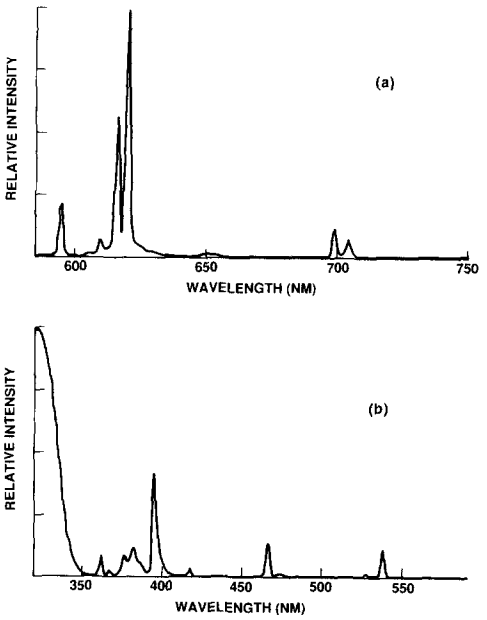

FIG. 9. Luminescence spectra for $EuVO_4$. (a) Emission spectrum with excitation wavelength at 393 nm; (b) excitation wavelength with emission wavelength at 616 nm.

9a). Other prominent bands occur at 595, 699, and 704-nm. The excitation spectrum shows all the lines characteristic of Eu^{3+} but with an additional peak at 322 nm (Fig. 9b).

Figure 10 shows phosphorescence emission spectra recorded at 77 K for vanadium deposited on the aluminosilicate matrix. Figure 10a is for AAA (VC) and exhibits well-defined vibrational fine structure with resonances at 452, 474, 496, 520, 577, and 611 nm. After Sn addition and calcination, the signal intensity decreases by a factor of 4 and the resolution of fine structure is decreased (Fig. 10b). Finally, after steaming, all vibrational structure is lost and the intensity of the signal decreases by another factor of 4 (Fig. 10c).

Another useful diagnostic tool is the color of the sample which is highly dependent upon treatment (see Table 3).

DISCUSSION

Europium(III) is a $4f^6$ ion giving rise to the spectroscopic ground state term $^7F_0$. In fact, Eu^{3+} is the only trivalent lanthanide with a total angular momentum quantum number, J, equal to zero. In solution, this imposes many restrictions on the induced electric dipole transition probabilities (*5–7*). Assuming J to be a good quantum number, transitions to (J' excited states) $J' = 0$ are forbidden as are all transitions for which J' is odd. The selection rule for the generally much less intense magnetic dipole

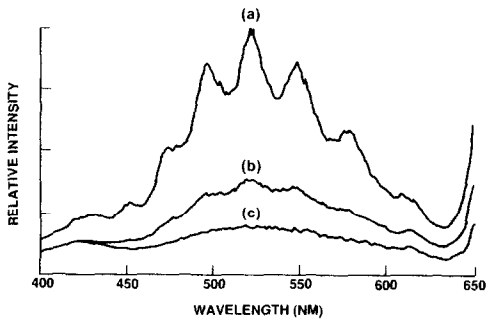

FIG. 10. Phosphorescence spectra recorded at 77 K with excitation wavelength at 320 nm for (a) AAA (VC), (b) AAA (VCSNC), and (c) AAA (VCSNCS).

TABLE 3

Sample Colors

Substrate	Treatment before steaming	Color before steaming[a]	Color after steaming[a]
EuY	C	W	W
	V	Br	Gr
	VC/VCSN	G	W
	VCSNC/SNCVC	OW	W
	VAAAC	G	W
	SN/SNC	W	W
	SNCV	Br	Br
	SNAAAC	W	W
	VCAAA	LG	LG
	SNCAAA	W	W
AAA	C	W	W
	V	Br	Br
	VC/VCSN	Gr	Gr
	VCSNC/SNCVC	Gr	Gr
	VYC	LG	W
	SN/SNC	W	W
	SNCV	Br	Br
	SNYC	W	W
	VCY	LG	LG
	SNCY	W	W
EuY/AAA	V	Br	Br
	VC/VCSN	Gr	Gr
	VCSNC/SNCVC	W/Gr	LG
	SN/SNC	W	W
	SNCV	Br	Br

[a] W, white; Br, brown; G, gray; OW, off-white; Gr, green; LG, light green.

transition is $\Delta J = 1$. An energy level diagram for Eu^{3+} is shown in Fig. 11 (*8*). At room temperature, the $^7F_1$ level is also partially populated, being only 360 cm^{-1} above the $^7F_0$ level, and so transitions from this state are also possible. Detailed calculations (*8*) have determined that for the aquo Eu^{3+} ion the only excitation transitions that are of appreciable intensity are $^7F_1 \rightarrow {}^5L_7$ and $^7F_0 \rightarrow {}^5L_6$ which should occur at 383 and 394 nm, respectively. Much weaker transitions occur for $^7F_1 \rightarrow {}^5G_5$, $^7F_1 \rightarrow {}^5L_6$, $^7F_1 \rightarrow {}^5D_3$, $^7F_1 \rightarrow {}^5L_7$, and $^7F_0 \rightarrow {}^5D_2$ at 380, 400, 416, 535, and 465 nm, respectively. A small transition at 525 nm corresponding to the magnetic dipole transition $^7F_0 \rightarrow {}^5D_1$ is also expected.

The excitation spectrum for "fresh" EuY exhibits a strong band at 393 nm and weaker bands at all the wavelengths listed above, indicating that the Eu^{3+} is in an aqueous environment even after exchange into the zeolite (Fig. 1a).

Emission spectra for Eu^{3+} ions usually exhibit transitions from $^5D_3$, $^5D_2$, $^5D_1$, and $^5D_0$ states to the 7*f* manifold (*9*). However, transitions from $^5D_3$, $^5D_2$, and $^5D_1$ are generally about a thousand times weaker than those from $^5D_0$. In hydrated EuY the three transitions $^5D_0 \rightarrow {}^7F_1$, $^5D_0 \rightarrow {}^7F_2$, and $^5D_0 \rightarrow {}^7F_4$ are observed with intensity ratios 1.2 : 1 : 0.7 (see Fig. 1b). Also, very weak bands corresponding to $^5D_0 \rightarrow {}^7F_3$ at 650 nm and $^5D_1 \rightarrow {}^7F_2$ at 554 nm are observed. These results are in good agreement with previous works on Eu^{3+} exchanged zeolites (*10, 11*).

After calcination, the intensity ratios of the emission and excitation bands for Eu^{3+} change significantly (Fig. 2a). The $^5D_0 \rightarrow {}^7F_2$ transition at 616 nm becomes the most intense band and the weak band at 650 nm corresponding to $^5D_0 \rightarrow {}^7F_3$ becomes

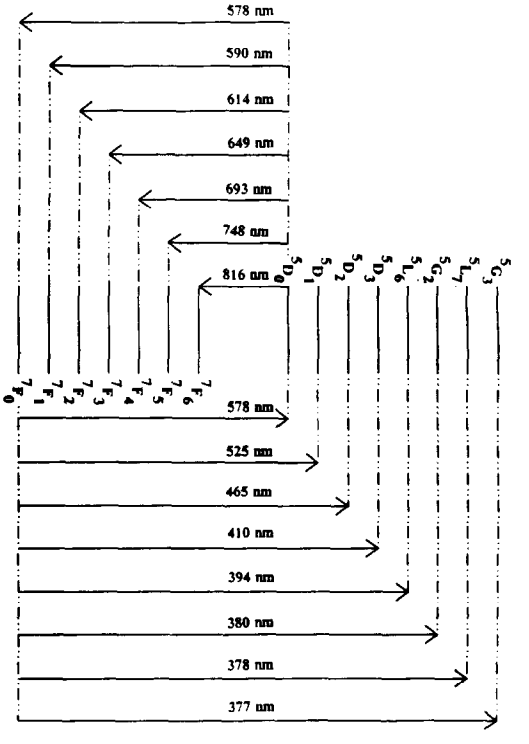

FIG. 11. Electronic energy levels for trivalent europium ions in solution. Adapted from Ref. (*8*).

stronger. Some vibrational fine structure is observed in the $^5D_0 \rightarrow {}^7F_2$ band with at least three observable components. Also, a sharp band at 578 nm corresponding to the $^5D_0 \rightarrow {}^7F_0$ transition is observed. More significantly, the excitation spectrum now shows major contributions from the following transitions $^7F_1 \rightarrow {}^5L_7$, 381 nm; $^7F_0 \rightarrow {}^5L_6$, 393 nm; $^7F_0 \rightarrow {}^5D_2$, 464 nm; $^7F_0 \rightarrow {}^5D_1$, 525 nm; $^7F_1 \rightarrow {}^5D_1$, 532 nm; $^7F_0 \rightarrow {}^5D_0$, 577 nm (see Fig. 2b). The appearance of previously nonallowed transitions is a result of a change in crystalline field which induces *J*-mixing whereby the *J* quantum numbers are no longer good. The energies of the transitions, however, remain almost constant due to the *f* electrons lying in nonbonding orbitals where they are highly shielded by the 5*s* electrons. This indicates that Eu^{3+} is no longer in an aqueous state but is probably coordinated to the zeolite lattice. The existence of the purely electric-dipole transitions $^5D_0 \rightarrow {}^7F_2$ and $^5D_0 \rightarrow {}^7F_0$ indicates that the Eu^{3+} species lacks inversion symmetry (otherwise these transitions would be forbidden (*12*)) and, therefore, is in a configuration lower than C_{3v} symmetry (*13*). A possible species would be the previously proposed rare-earth hydroxyl bridges which span the sodalite cages (*14*).

Addition of $Sn(Ph_4)$ followed by calcination to remove the phenyl ligands has very little effect on the europium luminescence (Fig. 3a). However, addition of vanadyl naphthenate both before and after calcination results in substantial quenching of the Eu^{3+} signal (Figs. 3b and 3c). This is further evidenced by the difference in the luminescence lifetime decays collected near 620 nm (353 ms vs 153 ms) for the Sn- and V-loaded EuY crystals, respectively. It is known from electron paramagnetic resonance evidence (*18*) that at this stage vanadium is mainly in the form of vanadyl (VO^{2+}) cations with the vanadium in a pseudo-octahedral crystal field. The energy transitions in such a species must be close in energy to those for Eu^{3+} in order for a transferral of energy between Eu^{3+} and the VO^{2+} cation. Also, the fact that luminescence quenching is so complete suggests that the VO^{2+} ions are distributed evenly through the zeolite.

Vanadyl sulfate solutions were used to exchange VO^{2+} ions into EuY in order to obtain further information concerning the quenching effects of VO^{2+} ions on Eu^{3+} luminescence. The VO^{2+} ions introduced via ion exchange were equally effective in quenching Eu^{3+} luminescence. On V-loaded EuY, the concentration of V_2O_5 is negligible at all stages. This is in agreement with the white or off-white color of the zeolite rather than the characteristic green color of V_2O_5 as shown in Table 3. These data also reinforce the conclusion that vanadium on the zeolite, prior to steaming, is present mainly as VO^{2+} cations.

After calcination of the vanadium-containing zeolite samples, the excitation spectrum exhibited an extra signal at 320 nm (Fig. 3c). This feature is fairly broad and is characteristic of $EuVO_4$, as seen in Fig. 9b. Emission bands for pure $EuVO_4$ are much narrower than those observed in catalyst systems, suggesting that $EuVO_4$ is only one of several environments for the europium in these samples. $EuVO_4$ formation is not hindered by the presence of Sn (see Fig. 7b).

The effects of luminescence quenching are very useful in determining migration properties of vanadium. When vanadium is loaded onto EuY and the zeolite mixed with AAA-alumina, the quenching effect remains even after calcination. This indicates that a large proportion of the vanadium has remained on the zeolite. When the vanadium-loaded AAA-alumina is mixed with EuY and calcined, luminescence quenching is negligible and $EuVO_4$ formation was not observed, indicating that vanadium did not migrate from the initial substrate (Fig. 4a). In contrast, when the vanadium-loaded AAA and EuY mixture is steamed, a large concentration of $EuVO_4$ is formed, indicating vanadium migration between substrates during steaming but not during calcination (Fig. 4b). When vanadium is loaded directly

onto the AAA-EuY mixture, luminescence intensity decreases by a factor of 3 from calcined EuY. A decrease by a factor of 2 can be attributed to the fact that the system has been diluted in half with one part containing no Eu^{3+}. Therefore, the Eu^{3+} luminescence quenching is minimal suggesting that the bulk of the vanadium has been preferentially deposited on the gel; vanadium deposition on the zeolite causes substantial quenching. Thus, the amorphous substrate has acted as a partial scavenger for vanadium. The colors of the samples given in Table 3 also reflect this property. Vanadium deposited on EuY and calcined is gray, whereas vanadium deposited on the gel alone or on the gel/EuY mixture is green, indicating V_2O_5 formation on these latter two substrates.

Formation of V_2O_5 on AAA-alumina is verified by the observance of a characteristic phosphorescence emission spectrum for V_2O_5 (*15, 17*) (Fig. 10). From the separation of the 0–0 (452 nm) and 0–1 (474 nm) transitions (vibrational state of the excited state to the vibrational state of the ground state), which is 1027 cm^{-1}, a V=O bond length may be calculated using the relationship: bond length (Å) = 2.751 − 0.00115 × wavenumber (cm^{-1}) (*17*). The bond length calculated is 1.57 Å which is in good agreement with the V=O bond length in pure V_2O_5 and 1.55–1.85 Å in silica-supported V_2O_5 (*27*). After Sn addition to AAA (VC) followed by calcination, the concentration of V_2O_5 diminishes by a factor of about 4; steaming further reduces the V_2O_5 concentration.

Addition of $Sn(Ph)_4$ to the vanadium-loaded zeolite and calcination (to remove the phenyl ligands) resulted in the quenching of the Eu^{3+} signal (Figs. 3b and 3c). Moreover, the Eu^{3+} luminescence spectra for EuY (VCSNC) and for EuY (SNCVC) are very similar to those for calcined, vanadium-free, EuY crystals. This suggests that after tin addition, the electronic energy levels of the vanadium are no longer of the correct energies to allow energy transfer between VO^{2+} and Eu^{3+} ions. This could be a result of a change in oxidation state of vanadium since it is believed from electron paramagnetic resonance (EPR) evidence (*18*) that most of the vanadium is V^{5+} at this stage or this could be a result of complexing of the vanadium with Sn or Eu. Since Eu^{2+} cations are not observed by EPR or luminescence, electron transfers are probably not occurring. Luminescence of Eu^{2+} near 440 nm, not observed here, has been readily observed in clays and zeolites (*20, 21*).

The order of deposition of Sn and V (Figs. 5 and 3c) has little effect on Eu^{3+} luminescence and the EuY (VCSNC) and EuY (SNCVC) samples have the same white color suggesting that V–Sn interactions in both zeolites are probably similar. After deposition of both tin and vanadium on the gel, a green color results suggesting the presence of V_2O_5.

All steamed samples exhibited very similar emission spectra (Figs. 6a and 8a); emission spectra of these materials are far less sensitive than excitation spectra to the environment of the Eu^{3+} cation. Nevertheless, some information about the symmetry of the Eu^{3+} species in the steamed samples may be obtained from excitation spectra. Figure 6a indicates the presence of a $^5D_0 \rightarrow {}^7F_0$ transition which suggests a lack of a center of inversion. Also, the $^5D_0 \rightarrow {}^7F_2$ band is split into at least three, possibly four or five, components and the broad nature of the $^5D_0 \rightarrow {}^7F_1$ band suggests unresolved fine structure. This splitting is due to a lifting of the degeneracy of the *J*-levels by the crystal field. The extent of the splitting suggests a low crystal symmetry, probably as low as C_2 (*11, 17, 19*). These data suggest that there are few (possibly one) environments for the Eu^{3+} after steaming.

The steamed samples' luminescence excitation spectra fall into three categories. The first is vanadium-free EuY samples. The second is vanadium-free AAA-alumina or AAA-EuY mixtures. The intensity ratios for these two cases are only subtly differ-

ent. Nevertheless, there is an interesting effect of the AAA-alumina on the environment of the Eu^{3+} cations in the mixed system. It seems unlikely that the AAA-alumina in the mixture could have a direct effect on Eu^{3+} cations buried within the zeolite particles. Therefore, either Eu^{3+} cations near the external surface of the zeolite are influenced by the gel after steaming or long-range effects via dipole coupling must be important.

The third type of Eu^{3+} excitation spectrum exhibits a new, broad excitation band centered at around 350 nm due to the presence of V. The intensity of the excitation band at 320 nm is two orders of magnitude greater after steaming than before suggesting that much more $EuVO_4$ (Figs. 7b and 9b) is formed at this stage. Once again, the presence of Sn does not prevent $EuVO_4$ formation. Indeed the greater the concentration of Sn the greater the concentration of $EuVO_4$ (see Fig. 8). The increase in the intensity of the 320-nm excitation is a true indication of the relative concentration of $EuVO_4$ because the lifetimes of the samples treated with variable tin concentration are similar. If quenching effects were important, then the lifetimes (both are 850 μs) would be different. It has been reported that tin concentrations between 0.2 and 2.5 wt% are effective in preventing breakdown of the zeolite structure and preserve cracking activity (*4*). Addition of too much tin, however, may have the opposite effect since, as shown here, it seems to favor $EuVO_4$ formation. A summary of the information learned from our luminescence experiments is given in Scheme II.

CONCLUSIONS

Europium(III) cations in fresh EuY crystals are in an aqueous environment. After calcination, they become anchored to the zeolite lattice possibly in the form of hydroxyl bridges. Vanadium addition to EuY

$EuY \xrightarrow[\text{Calcine, 540°C}]{} EuY\ (C)$	[Eu^{3+} in low symmetry site, $<C_2$, Eu^{3+} in sodalite cages]
$EuY \xrightarrow[\text{V naph.}]{} EuY\ (V)$	[V naph. on zeolite, emiss. 350 nm]
$EuY\ (V) \xrightarrow[\text{Calcine 540°C}]{} EuY\ (VC)$	[Some V_2O_5 on zeolite, emiss. 520 nm; some $EuVO_4$, exc. 320 nm]
$EuY\ (VC) \xrightarrow[\text{Steam, 730°C}]{} EuY\ (VCS)$	[>90% V is V_2O_5, emiss. 520 nm; some $EuVO_4$, exc. 320 nm]
$AAA\ (V) \xrightarrow[\text{EuY, Calcine 540°C}]{} AAA\ (VYC)$	[Eu^{3+} ions in zeolite, emiss. 616 nm]
$AAA\ (VYC) \xrightarrow[\text{Steam, 730°C}]{} AAA\ (VYCS)$	[$EuVO_4$ formation, exc. 320 nm; migration of V from AAA to Y]
$AAA\ (V) \xrightarrow[\text{Calcine, 540°C}]{} AAA\ (VC)$	[V_2O_5 formation, emiss. 520 nm]
$EuY\ (VCSN) \xrightarrow[\text{Calcine, 540°C}]{} EuY\ (VCSNC)$	[less V_2O_5 after Sn addition, emiss. 520 nm]
$EuY\ (VCSNC) \xrightarrow[\text{Steam, 730°C}]{} EuY\ (VCSNCS)$	[no vibrational structure at 520 nm, V_2O_5-like environment, some $EuVO_4$, Sn–O–V_2O_5 interaction]
$AAA\ (VCSNC) \xrightarrow[\text{Steam, 730°C}]{} AAA\ (VCSNCS)$	[no vibrational structure at 520 nm, V_2O_5-like environment, Sn–O–V_2O_5 interaction]

SCHEME II. Summary of results of luminescence studies.

results in a VO^{2+} species which interacts with Eu^{3+} cations, quenching the Eu^{3+} luminescence. Vanadium deposited initially on either EuY or AAA-alumina does not migrate to the other substrate upon calcination but does migrate upon steaming. Luminescence may be used, therefore, to track metals migration. Migration of Ni and V on equilibrium FCCs has recently been tracked using imaging secondary ion mass spectrometry methods (*22*). On EuY/AAA mixtures, vanadium is preferentially sorbed by the gel. Prior to steaming, vanadium is present on the gel primarily in the form of V_2O_5 whereas on the zeolite it is present as VO^{2+} ions.

All the steamed samples contain an Eu^{3+} species with a very low symmetry, less than C_2; vanadium on EuY crystals forms $EuVO_4$. Sharp luminescence bands indicate that neither site disorder nor a multitude of europium environments is present. Scanning transmission electron microscopy experiments in combination with energy dispersive X-ray analyses have been used to independently observe the formation of $LaVO_4$ in LaY systems (*23*). The concentration of $EuVO_4$ is very low after calcination but increases significantly after steaming. The order of deposition of vanadium and tin on both EuY or AAA-alumina is irrelevant. The presence of Sn removes Eu^{3+}–VO^{2+} interactions either by oxidizing the vanadium or by forming a tin–vanadium or vanadium–europium complex. Tin is believed to complex vanadium and excess Sn seems to encourage formation of $EuVO_4$. Thus, excess tin is to be avoided when this metal is used to passivate vanadium.

ACKNOWLEDGMENTS

The authors thank J. F. Tanguay for assistance in recording luminescence lifetime measurements. We thank the donors of the Petroleum Research Fund of the American Chemical Society for support of this research.

REFERENCES

1. Occelli, M. L., *in* "Fluid Catalytic Cracking: Its Role in Modern Refining" (M. L. Occelli, Ed.), ACS Symposium Series 375, p. 1. Amer. Chem. Soc., Washington, DC, 1988.
2. (a) Murphy, J. R., *in* "Sym., Prod., Character., Process. of Heavy Oils," p. 5. University of Utah, 1981; (b) Gall, J. W., NPRA Annual Meeting, Paper No. AM82-50, p. 5, 1982.
3. Meisenheimer, R. G., *J. Catal.* **1,** 356 (1962).
4. English, A. R., and Kowalczyk, D. C., *Oil Gas J.,* 127 (1984).
5. Carnall, J. W., Fields, P. R., and Rajnak, K., *J. Chem. Phys.* **49,** 4412 (1968).
6. Jorgensen, C. K., and Reisfeld, R., *J. Less-Common Met.* **93,** 107 (1983).
7. Ofelt, G. S., *J. Chem. Phys.* **37,** 511 (1962).
8. Carnall, W. T., Fields, P. R., and Rajnak, K., *J. Chem. Phys.* **49,** 4450 (1968).
9. VanClitert, L. G., Linares, R. C., Soden, R. R., and Bellman, A. A., *J. Chem. Phys.* **36,** 702 (1962).
10. Tanguay, J. F., and Suib, S. L., *Catal. Rev. Sci. Eng.* **29,** 1 (1987).
11. Pott, G. T., and Stork, W. H. J., *Catal. Rev. Sci. Eng.* **12,** 163 (1975).
12. Blasse, G., and Bril, A., *J. Chem. Phys.* **45,** 3327 (1966).
13. Richardson, F. S., and Brittain, H. G., *J. Amer. Chem. Soc.* **103,** 18 (1981).
14. Olson, D. H., Kokotailo, G. T., and Charnell, J. F., *J. Colloid Interface. Sci.* **28,** 305 (1968).
15. Occelli, M. L., Psaras, D., and Suib, S. L., *J. Catal.* **96,** 363 (1985).
16. Ronde, H., and Blasse, G., *J. Inorg. Nucl. Chem.* **40,** 215 (1978).
17. Iwamoto, M., Furukawa, H., Matsukami, K., Takenaka, T., and Kagawa, S., *J. Amer. Chem. Soc.* **105,** 3719 (1983).
18. (a) Anderson, M. W., Occelli, M. L., and Suib, S. L., submitted for publication; (b) Wachs, I., *Mater. Res. Soc. Symp. Proc.* **111,** 353 (1988); (c) Woolery, G. L., Chin, A. A., Kirker, G. W., and Huss, A., *in* "Fluid Catalytic Cracking" (M. L. Occelli, Ed.), ACS Symposium Series 375, pp. 215–228. Amer. Chem. Soc., Washington, DC, 1988.
19. Suib, S. L., and Carrado, K. A., *Inorg. Chem.* **24,** 200 (1985).
20. Bergaya, F., and VanDamme H., *J. Chem. Soc. Faraday Trans. 2* **79,** 505 (1983).
21. (a) Arakawa, T., Takakuwa, M., and Shiakawa, J., *Bull. Chem. Soc. Japan* **57,** 948 (1984); (b) Arakawa, T., Takata, T., Takakuwa, M., Adachi, G. Y., and Shiakawa, J., *Mater. Res. Bull.* **17,** 171 (1982).
22. Kugler, E. L., and Leta, D. P., *J. Catal.* **109,** 387 (1988).
23. Mauge, F., Courcelle, J. C., Engelhard, Ph., Gallezot, P., and Grosmangin, J., *in* "Proceedings, 7th Int. Zeolite Conf., Tokyo" (Y. Murakami, A. Iijima, and J. W. Ward, Eds.), p. 803, 1986.